



## Catalytic activity of the $\text{SO}_4^{\bullet-}$ radical for photodegradation of the azo dye Cibacron Brilliant Yellow 3 and 3,4-dichlorophenol: Optimization by application of response surface methodology

María C. Yeber\*, L. Díaz, J. Fernández

Catholic University of the Santísima Concepción, Faculty of Sciences, Alonso de Ribera 2850, casilla 297 Concepción, Chile

### ARTICLE INFO

#### Article history:

Received 14 January 2010

Received in revised form 21 June 2010

Accepted 22 July 2010

Available online 1 August 2010

#### Keywords:

Advanced oxidation process

Azo dyes

Persulfate

Brilliant Yellow 3

Cibacron

$\text{SO}_4^{\bullet-}$

3,4-Dichlorophenol

### ABSTRACT

Advanced oxidation processes (AOP) generate in situ active radicals with a high oxidation potential, allowing for the destruction of polluting agents through organic compound mineralization. The use of experimental design is a tool that allows adjustment of factors to obtain an optimal response in experimental analysis. We used multivariate analysis to optimize the process of organic removal from wastewater in a cylindrical reactor, using UV radiation (254 nm) and peroxodisulfate as an oxidant. We used 3,4-dichlorophenol and Cibacron Brilliant Yellow 3 (CBY-3) as model organic compounds. Both of these compounds are characteristic polluting agents present in industrial wastewater. We used a factorial  $2^n$  design to obtain the best experimental conditions to efficiently remove the compounds from the solution, using time and oxidant concentration as experimental variables. The initial concentration of both compounds was 100 ppm, and we obtained 90% dichlorophenol removal, with a rate constant of  $0.0386 \text{ min}^{-1}$ . Degradation of azo dye was more efficient reaching 98%, with a rate constant of  $0.0908 \text{ min}^{-1}$ . In both cases, the optimal time for reducing the maximum concentration was 60 min of irradiation. Total organic carbon (TOC) reduction was analyzed to determine the efficiency of the UV/ $\text{K}_2\text{S}_2\text{O}_8$  process in mineralization, where we obtained 90% TOC reduction for both organic compounds. At the same time, the dye compound, CBY-3, whose organic structure is more complex, generated nitrate and chloride ions as mineralization products. The efficient mineralization of both compounds is based on the in situ formation of the strong oxidant sulfate anion radical ( $E = 2.5\text{--}3.1 \text{ V}$ ).

© 2010 Elsevier B.V. All rights reserved.

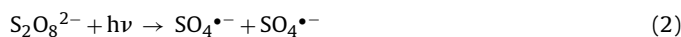
### 1. Introduction

Chlorophenol compounds have been widely used as insecticides, fungicides, herbicides, algacides and antiseptics, as well as intermediaries in the production of dyes, plastics and pharmaceuticals. Furthermore, they can be produced by the environmental degradation of more complex molecules, such as phenoxyacetic acids and chlorobenzenes [1–3]. One important source of chlorophenols is the bleaching process in the pulp and paper industry, which uses chlorine dioxide to generate chlorinated phenols by reaction of the residual lignin, which is chemically linked to the cellulose, forming compounds which have been described in the literature as bioaccumulable toxins with high carcinogenic potential [4–7].

Different oxidation technologies for the treatment of effluents have been described in the literature, such as ozone, or semiconductors combined with UV light [8–10], and hydrogen peroxide

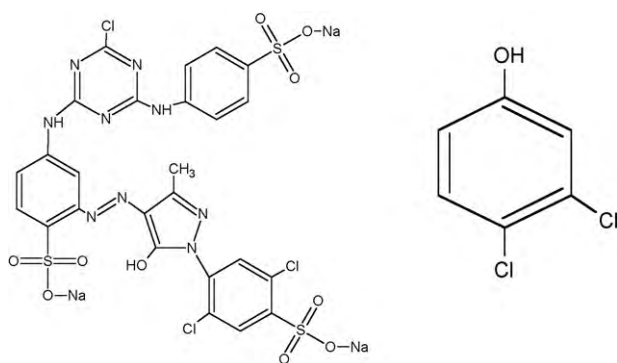
[11,12]. These treatments obtain effluent degradation under different conditions, reducing environmental parameters, such as biological oxygen demand (BOD), chemical oxygen demand (COD), total organic carbon (TOC), and organochlorine compounds (AOX), therefore reducing acute toxicity [13,14].

Azo dyes constitute an important group of organic compounds, characterized by presenting one or more azo bonds ( $-\text{N}=\text{N}-$ ). These organic compounds are widely used in numerous industries, such as textiles, food, cosmetics, and paper printing [15,16]. The environmental impact caused by effluents containing these organic compounds is varied, and classic methods for their elimination have not been efficient in achieving low partial oxidations or reductions, generating highly toxic secondary products. Oxidation technologies using activation of persulfate results in the in situ formation of the sulfate radical ( $\text{SO}_4^{\bullet-}$ ) under a broad range of pH ( $1 \leq \text{pH} \leq 10.5$ ) [17]. Therefore, persulfate can be activated by electron transfer (Eq. (1)) or by photolysis (Eq. (2)) [18–20].



\* Corresponding author. Tel.: +56 41 2735250; fax: +56 41 2735251.

E-mail address: [mcyeber@ucsc.cl](mailto:mcyeber@ucsc.cl) (M.C. Yeber).



Scheme 1. Structures of Cibacron BY-3 and 3,4-dichlorophenol.

The sulfate radical has a wide range of optical absorption, with a maximum of 450 nm,  $\epsilon = 1100 \text{ Ls mol}^{-1} \text{ cm}^{-1}$ , and is a strong oxidant, with a redox potential between 2.6 and 3.1 V, relative to the normal hydrogen electrode (NHE) [21]. It reacts with many organic compounds and is as efficient an oxidant as the  $\bullet\text{OH}$  radical, which can react as fast through hydrogen abstraction. In addition, this radical oxidizes chloride ions in solutions near neutrality, being advantageous for the production of  $\text{Cl}_2^{\bullet-}$ , which is difficult to achieve with hydroxyl radicals [22].

## 2. Experimental

### 2.1. Photocatalytic process

We carried out photochemical oxidation using the  $\text{K}_2\text{S}_2\text{O}_8/\text{UV}$  system at neutral pH, using two representative compounds of industrial wastewater: 3,4-dichlorophenol and Cibacron BY-3 (Scheme 1), for which 100 ppm treatments of each solution were prepared. The removal of compounds from the solution was followed using a spectrophotometer (Shimadzu UV – 1601). All reagents were Merck quality.

### 2.2. Experimental design

The experimental design was constructed using two coded values for each variable, maximum (+1) and minimum (–1), and  $n$  factors. The minimum number of tests was  $2^n$ . The model allows the construction of contour plots, and the prediction of values at any point in the region of interest. The equations obtained from the model are expressed by a second order polynomial function (Eq. (3))

$$Y(\%) = \beta_0 + \sum_{i,j=1}^n K_i X_i + \sum_{i,j=1}^n K_j X_j^2 + \sum_{i,j=1}^n K_{ij} X_i X_j \quad (3)$$

where  $\beta_0$  = average value of the experimental response;  $K_i$  = main effect of the coded variable  $X_i$ ;  $K_{ij}$  = quadratic effect of the coded variable  $X_j$ ;  $K_{ij}$  = interaction effects between the respective coded variables.

An experimental full quadratic matrix was designed for each compound (Tables 1 and 2), using the statistical program Modde 7.0, to determine the optimal experimental variables: time (in min) and peroxodisulfate (in g). Each table shows the experimental matrix obtained from the model with the coded and uncoded values, and the order in which the experiments were carried out. Photochemical oxidations were performed in a tubular quartz reactor with an HPL-UV-C mercury lamp (254 nm, 120 W).

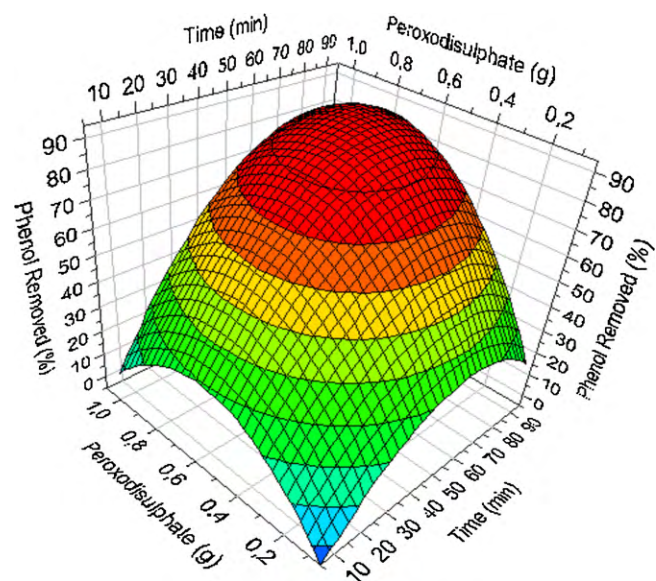


Fig. 1. Response surface for the experimental design for 3,4-dichlorophenol.

### 2.3. Measurement of analytical parameters

We made spectrophotometric and colorimetric determination of organic matter mineralization products in a Spectroquant NOVA 60 Merck. Chloride ion analysis was determined by the 325, 1 EPA norm and the Standard U.S. Method 4500. Nitrate analysis was carried out using the DIN 38405 D9 and ISO 7890/1 method, given that in a solution acidified with sulfuric and phosphoric acid, nitrate reacts with 2,6-dimethylphenol to form orange colored 4-nitro-2,6-dimethylphenol, which is determined photometrically at 338 nm. Nitrite was also determined photometrically at 525 nm using EPA 354.1, U.S. Standard Methods 4500- $\text{NO}_2^-$  B, ISO 6777 and IN 26777, based reaction with sulphanic acid and N-1 - naphthylethylenediamine dihydrochloride, which forms a magenta azo dye (Griess' reaction). For TOC analysis the samples were filtered with cellulose 0.22  $\mu\text{m}$  filters, acidified with hydrochloric acid, and injected in a TOC analyzer (Shimadzu 5000).

## 3. Results and discussion

We carried out the optimization process using the  $\text{K}_2\text{S}_2\text{O}_8/\text{UV}$  photocatalytic system for oxidation of 3,4-dichlorophenol and Cibacron BY-3, in order to compare the effect of the system on two organic compounds with different molecular structures, which are generally present in diverse industrial effluents. Tables 1 and 2, respectively, show the coded experimental variables, the order in which the experiments were run, and number of experiments. In addition, the corresponding observed and predicted responses for the optimization of organic compound degradation for each case are observed in the corresponding tables. Based on the difference between observed and predicted responses, the model determined the experimental error with a 95% confidence interval.

Once the experimental matrices were generated with their respective responses, the experimental variables were combined, thus obtaining a three-dimensional surface. In these plots the synergism between the experimental variables can be observed, resulting in an optimal zone, where it is possible to identify the values of the variables given by the model which result in the optimal response. The response surface of 3,4-dichlorophenol (Fig. 1) indicates that the optimal time for the efficient removal of the compound is observed at 40 min, with 0.7 g of oxidant. In the case of the CBY-3 dye (Fig. 3), the optimal time is observed at 40 min, with

**Table 1**

Experimental matrix of the variables, with corresponding experimental and predicted responses to optimize 3,4-dichlorophenol removal.

Exp.	Run exp.	Time (min)	K <sub>2</sub> S <sub>2</sub> O <sub>8</sub> (g L <sup>-1</sup> )	3,4-Dichlorophenol removed (%) Observed response	3,4-Dichlorophenol removed (%) Predicted response
N1	6	5.0 (-1)	0.05 (-1)	11.40	3.17
N2	1	47.5 (0)	0.05 (-1)	10.79	14.84
N3	2	90.0 (+1)	0.05 (-1)	22.32	26.50
N4	5	5.0 (-1)	0.525 (0)	8.91	46.09
N5	10	47.5 (0)	0.525 (0)	80.54	70.44
N6	12	90.0 (+1)	0.525 (0)	82.42	94.79
N7	7	5.0 (-1)	1.0 (+1)	10.22	15.02
N8	9	47.5 (0)	1.0 (+1)	74.06	52.05
N9	3	90.0 (+1)	1.0 (+1)	71.87	89.08
N10	4	47.5 (0)	0.525 (0)	89.34	70.45
N11	8	47.5 (0)	0.525 (0)	87.90	70.44
N12	11	47.5 (0)	0.525 (0)	73.52	70.44

**Table 2**

Experimental matrix of the variables, with corresponding experimental and predicted responses to optimize Cibacron BY-3 removal.

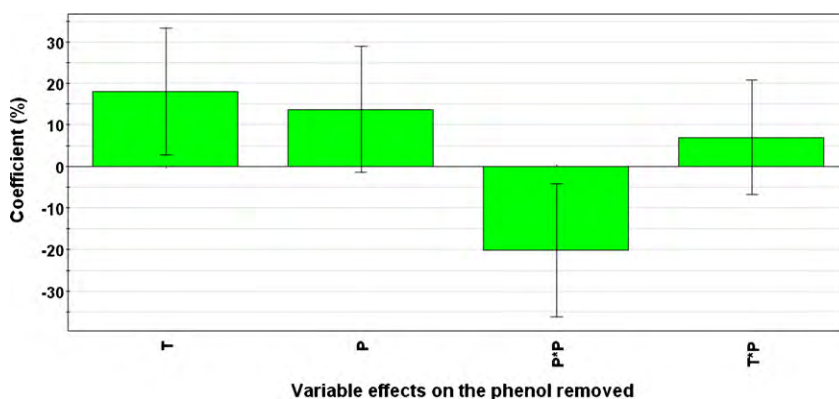
Exp.	Run exp.	Time (min)	K <sub>2</sub> S <sub>2</sub> O <sub>8</sub> (g L <sup>-1</sup> )	Cibacron removed (%) Observed response	Cibacron removed (%) Predicted response
N1	6	15.0 (-1)	0.1 (-1)	44.49	47.56
N2	1	37.5 (0)	0.1 (-1)	81.65	78.95
N3	2	60.0 (+1)	0.1 (-1)	93.71	93.34
N4	5	15.0 (-1)	0.55 (0)	80.75	77.42
N5	10	37.5 (0)	0.55 (0)	98.72	98.49
N6	12	60.0 (+1)	0.55 (0)	99.01	100.0
N7	7	15.0 (-1)	1.0 (+1)	90.51	90.77
N8	9	37.5 (0)	1.0 (+1)	98.61	100.0
N9	3	60.0 (+1)	1.0 (+1)	98.46	95.28
N10	4	37.5 (0)	0.55 (0)	99.06	98.49
N11	8	37.5 (0)	0.55 (0)	97.35	98.49
N12	11	37.5 (0)	0.55 (0)	99.03	98.49

0.5 g of oxidant. By statistically solving the experimental matrix, the following polynomial modeling equations were developed, each giving rise to the response surface. The modeling equations were developed so that the importance of the parameters in the mathematical solution is obtained from the experimental design, with respect to the weight of each variable. Thus, an empirical relationship between the response and the variables is expressed by the polynomial equation, in this case for 3,4-dichlorophenol (Eq. (4)) and for Cibacron BY-3 (Eq. (5)), where *Y* represents the percentage of the compounds removed, *X*<sub>1</sub> is the reaction time in min, and *X*<sub>2</sub> is peroxydisulfate in g.

$$Y(\%) = 79(\pm 2.5) + 18(\pm 1.6)X_1 + 13(\pm 1.6)X_2 - 13.9(\pm 1.5)X_1^2 - 15.4(\pm 1.8)X_2^2 + 6.9(\pm 1.6)X_1X_2 \quad (4)$$

$$Y(\%) = 98.5(\pm 1.5) + 12.6(\pm 1.3)X_1 + 11.3(\pm 1.3)X_2 - 8.5(\pm 1.9)X_1^2 - 8.2(\pm 1.9)X_2^2 - 10.3(\pm 1.6)X_1X_2 \quad (5)$$

Statistical analyses determined that the quadratic effects of the variables were significant in the response, where the polynomial equation represented the response influenced by synergism between variables, reaction time and oxidant concentration. Fig. 2 shows the influence of each variable on the response, and the correlation coefficient values (in percentage) for the statistics, with a 95% confidence interval. In the case of Cibacron BY-3, as is observed in Fig. 4, the efficiency of reduction was directly influenced by the synergism between the time of the reaction and oxidant concentration. The catalyst had the largest positive effect on the responses, and

**Fig. 2.** Analysis of the influence of parameters on 3,4-dichlorophenol removal, with a 95% confidence interval.

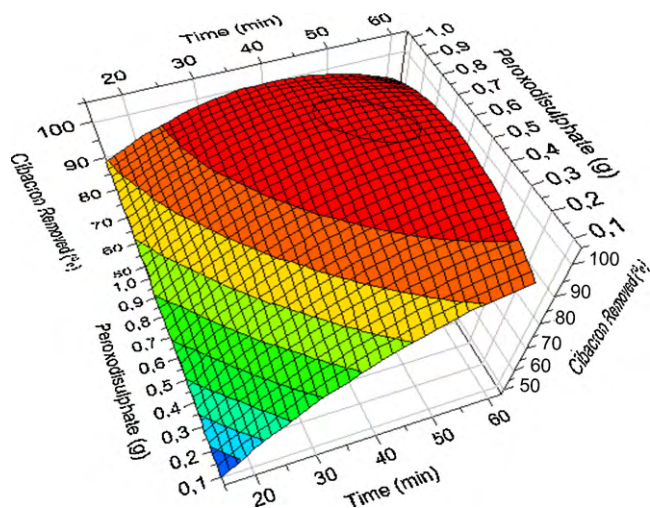


Fig. 3. Response surface of the experimental design for Cibacron BY-3.

the second degree terms were not significant for both responses (Figs. 2 and 4).

Both models are statistically evaluated as valid, given the high values of  $R^2$  (0.96) and  $Q^2$  (0.78), observed for Cibacron BY-3, and  $R^2$  (0.97) and  $Q^2$  (0.80) observed for 3,4-dichlorophenol, which means that the regression model provides a good description of the relationship between the independent variables and the response. Here  $R^2$  represents the fraction of the variation of the response explained by the model, and  $Q^2$  is the fraction of the variation of the response that can be predicted by the model, resulting in the statistical validity of the full quadratic model with  $p < 0.001$ .

### 3.1. Photochemical process

The optimal conditions identified for the removal of 3,4-dichlorophenol and Cibacron BY-3 were experimentally validated by following the kinetics of the reaction, as is shown in Fig. 5. Peroxodisulfate activated by UV-C light during the photolysis process generated in situ sulfate radicals ( $\text{SO}_4^{\bullet-}$ ), which are a highly reactive species responsible for the oxidation process [23,24]. Analysis of the kinetics showed a rapid decrease in concentration in the case where the azo dye is treated photocatalytically, resulting in nearly 100% removal after 40 min of treatment. Phenol compound removal was lower, which coincides with the optimal points of the variables obtained in the analysis of the contour plots and the polynomial equation. The value obtained for the reaction rate constant was  $0.0908 \text{ min}^{-1}$  for Cibacron BY-3 and  $0.0386 \text{ min}^{-1}$  for 3,4-

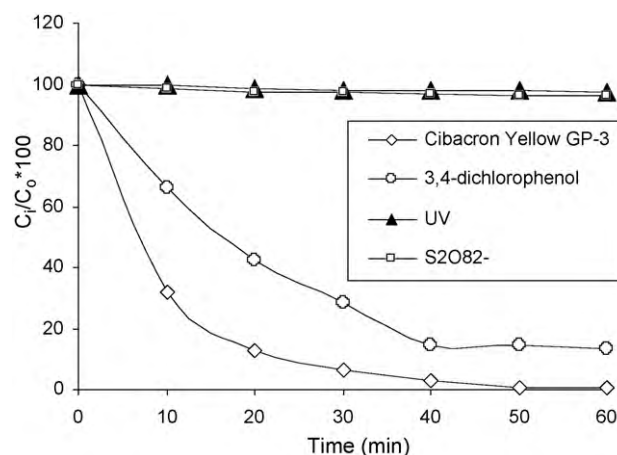


Fig. 5. Cibacron BY-3 and 3,4-dichlorophenol kinetics using the optimized  $\text{K}_2\text{S}_2\text{O}_8/\text{UV}$  systems.

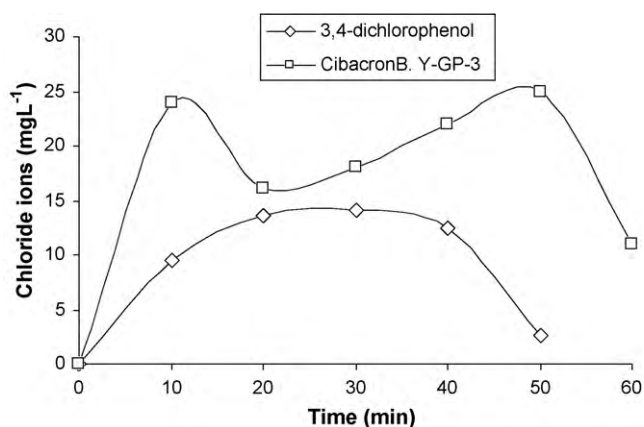


Fig. 6. Chloride ions generated during Cibacron BY-3 and 3,4-dichlorophenol degradation using the optimized  $\text{K}_2\text{S}_2\text{O}_8/\text{UV}$  systems.

dichlorophenol, corroborating kinetic analysis. Both compounds contain strong electron attraction given the presence of chloride groups in their molecular structure. Due to their high electronegativity, these are attacked by sulfate radicals through nucleophilic addition, increasing the chloride ions in the solution during the oxidation process. Chloride ion concentration generated during the photochemical process is illustrated in Fig. 6. The presence of chloride ions in the first minutes of the reaction indicates that the sulfate radicals attack atoms of carbon  $\beta$  and  $\gamma$ , eliminating chloride ions.

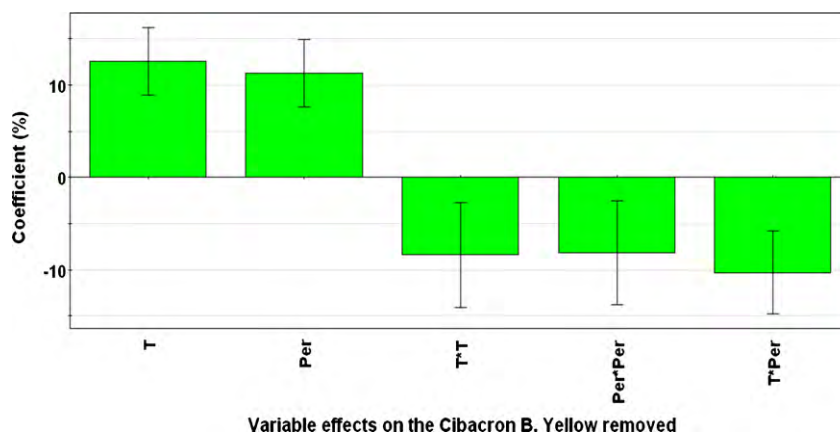


Fig. 4. Analysis the parameters influence over Cibacron BY-3 removal with 95% confidence.

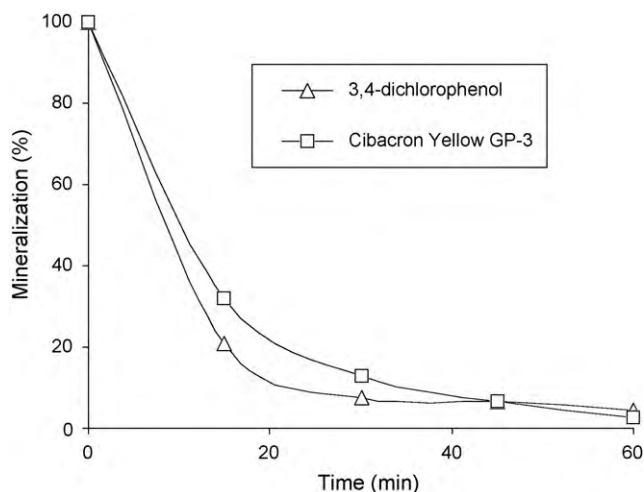


Fig. 7. Mineralization efficiency of 3,4-dichlorophenol and Cibacron BY-3 using the optimized oxidation process.

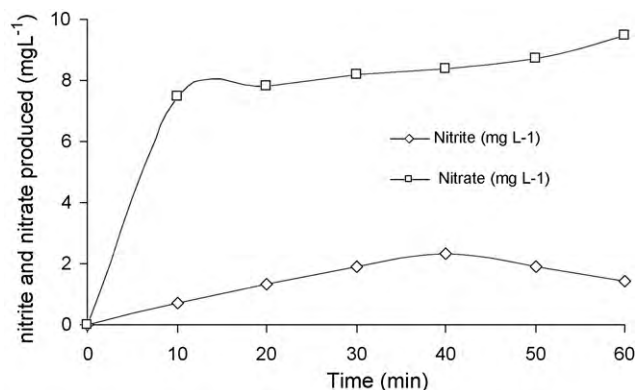


Fig. 8. Generation of nitrite and nitrate during the Cibacron BY-3 mineralization process.

In both cases, the chloride ions increase over time, reaching the maximum, and in the following minutes begin to decrease, indicating that the sulfate radicals begin to oxidize chloride ions until they become chlorine radicals (Eq. (6)). Higher chloride ion content in the solution promotes faster destruction of dyes due to the active formation of chlorine species [18]. Other researchers [25,26] have also reported the formation of chlorine radicals when chloride species are present in solution in the presence of sulfate radicals.



The efficiency of the  $\text{K}_2\text{S}_2\text{O}_8/\text{UV}$  process for mineralizing the organic compounds was analyzed using total organic carbon (TOC). Initial TOC was 44.27 ppm for phenol and 34.15 ppm for 3,4-dichlorophenol, in 100 ppm of solution. As is observed in Fig. 7, the profiles decrease rapidly, reaching 96% of total mineralization. These results agree with other work, where persulfate has been used in different processes as an oxidant in order to achieve organic compound degradation [27–31], demonstrating the efficiency of sulfate radicals in the oxidation process due to their higher oxidation potential, compared with hydroxyl radicals, as well as being highly stable in solution, and not presenting decomposition in the time, as is observed with hydrogen peroxide [32,33].

The CBY-3 azo dye is a complex molecular structure that contains chlorine and nitrogen atoms. Photochemical treatment generates mineralization, resulting in chloride ions, nitrites and nitrates (Fig. 8). The nitrite ion is formed rapidly, and is oxidized into nitrate, demonstrating [34,35] that the potential of sulfate radicals

is sufficient to oxidize nitrogen atoms to nitrate ions, also reducing TOC, indicating the efficiency for total organic matter mineralization.

Different advanced oxidation processes have appeared as interesting techniques for the treatment of organic pollutants [36–40,24]. Among the most used is the well-known heterogeneous photocatalysis. Indeed, titanium dioxide activation under UV irradiation allows the generation of highly reactive free hydroxyl radicals from the hydroxide ions of water [41–43]. In this study, it was possible to observe that the sulfate radicals generated in situ can be reactive, as well as the hydroxyl radicals, producing strong mineralization of both phenol and Cibacron. The efficiency of the developed process lies primarily in the high oxidizing strength of the sulfate radicals that are formed. The sulfate radicals are stronger oxidants than the hydroxyl radicals, especially at neutral pH, considering the comparison of their redox potentials [27]. On the other hand, the use of multivariate analysis allowed an accurate optimal response and an adequate statistical analysis [44,45].

#### 4. Conclusions

The advanced oxidation process using the  $\text{K}_2\text{S}_2\text{O}_8/\text{UV}$  system was efficient in the mineralization of 3,4-dichlorophenol and Cibacron BY-3. The in situ production of sulfate radicals and chloride ions during the reaction produced greater reduction of the compound, mainly in the case of the azo dye, where the concentration of the chloride ions in solution was highest, which could promote faster compound reduction. The use of experimental design demonstrates that this is a good tool for determining the efficiency of treatments with a statistically reliable analysis.

#### Acknowledgment

This research was supported by the Catholic University of the Santísima Concepción Grant DIN no. 03-2002 to MCY.

#### References

- [1] R. Valo, V. Kitunen, M. Salkinoja-Salonen, S. Räsänen, Chlorinated phenols as contaminants of soil and water in the vicinity of two Finnish sawmills, *Chemosphere* 13 (8) (1984) 835–844.
- [2] M. Czaplicka, Sources and transformations of chlorophenols in the natural environment, *Science of the Total Environment* 322 (2004) 21–39.
- [3] J. Gao, L. Liu, X. Liu, H. Zhou, S. Huang, Z. Wang, Levels and spatial distribution of chlorophenols – 2,4-dichlorophenol, 2,4,6-trichlorophenol, and penta-chlorophenol in surface water of China, *Chemosphere* 71 (6) (2008) 1181–1187.
- [4] B. Bukowska, 2,4,5-T and 2,4,5-TCP induce oxidative damage in human erythrocytes: the role of glutathione, *Cell Biology International* 28 (7) (2004) 557–563.
- [5] J. Zhang, H. Shen, X. Wang, J. Wu, Y. Xue, Effects of chronic exposure of 2,4-dichlorophenol on the antioxidant system in liver of freshwater fish *Carassius auratus*, *Chemosphere* 55 (2) (2004) 167–174.
- [6] S. Kamenev, J. Kallas, R. Munter, M. Trapido, Chemical oxidation of biologically treated phenolic effluents, *Waste Management* 15 (3) (1995) 203–208.
- [7] F. Reyes, S. Chamorro, M.C. Yeber, G. Vidal, Characterization of E1 Kraft Mill effluent by toxicity identification evaluation methodology, *Water, Air & Soil Pollution* 199 (2009) 183–190.
- [8] I.N. Martyanov, E.N. Savinov, V.N. Parmon, A comparative study of efficiency of photooxidation of organic contaminants in water solutions in various photochemical and photocatalytic systems. 1. Phenol photooxidation promoted by hydrogen peroxide in a flow reactor, *Journal of Photochemistry and Photobiology A: Chemistry* 107 (1–3) (1997) 227–231.
- [9] C. Lizama, M.C. Yeber, J. Freer, J. Baeza, H. Mansilla, Reactive dye decoloration by  $\text{TiO}_2$  photo-assisted catalysis, *Water Science and Technology* 44 (2001) 197–203.
- [10] S. Parra, S. Malato, C. Pulgarin, New integrated photocatalytic biological flow system using supported  $\text{TiO}_2$  and fixed bacteria for the mineralization of isopropruron, *Applied Catalysis B: Environmental* 36 (2002) 131–144.
- [11] W. Gernjak, T. Glaser, S. Malato, J. Caceres, R. Bauer, A. Fernandez, Photo-Fenton treatment of water containing natural phenolic pollutants, *Chemosphere* 50 (2003) 71–78.
- [12] J. Saien, M. Asgari, A.R. Soleymani, N. Taghavinia, Photocatalytic decomposition of Direct Red 16 and kinetics analysis in a conic body packed bed reactor with nanostructure titania rasching rings, *Chemical Engineering Journal* 151 (2009) 295–301.

- [13] M.C. Yeber, J. Rodríguez, J. Freer, J. Baeza, N. Durán, H.D. Mansilla, Advanced oxidation of a pulp mill bleaching wastewater, *Chemosphere* 39 (1999) 1679–1688.
- [14] A. Chiaviola, Textiles, *Water Environment Research* 81 (10) (2009) 1696–1730.
- [15] P. Seesuriyachan, T. Chaiyaso, K. Sasaki, C. Techapun, Influence of food colorant and initial COD concentration on the efficiencies of micro-aerobic sequencing batch reactor (micro-aerobic SBR) for casein recovery under non-sterile condition by *Lactobacillus casei* TISTR 1500, *Bioresource Technology* 100 (18) (2009) 4097–4103.
- [16] A. Pandey, P. Singh, L. Iyengar, Bacterial decolorization and degradation of azo dyes, *International Biodeterioration & Biodegradation* 59 (2) (2007) 73–84.
- [17] G.P. Anipsitakis, D.D. Dionysiou, Transition metal/UV-based advanced oxidation technologies for water decontamination, *Applied Catalysis B: Environmental* 54 (2004) 155–163.
- [18] K.L. Ivanov, E.M. Glebov, V.F. Plyusnin, Y.V. Ivanov, V.P. Grivin, N.M. Bazhin, Laser flash photolysis of sodium persulfate in aqueous solution with additions of dimethylformamide, *Journal of Photochemistry and Photobiology A: Chemistry* 133 (2000) 99–104.
- [19] L. Dogliotti, E. Hayon, Flash photolysis of persulfate ions in aqueous solutions. Study of the sulfate and ozonide radical anions, *The Journal of Physical Chemistry* 71 (1967) 2511–2516.
- [20] P. Neta, V. Madhavan, H. Zemel, R. Fessenden, Rate constants and mechanism of reaction of  $\text{SO}_4^{\bullet-}$  with aromatic compounds, *Journal of the American Chemical Society* 99 (1) (1977) 163–164.
- [21] M. Antoniou, A. de la Cruz, D. Dionysiou, Intermediates and reaction pathways from the degradation of microcystin-LR with sulfate radicals, *Environmental Science & Technology* (2010), doi:10.1021/es1000243.
- [22] D. Wang, Y. Li, M. Yang, M. Han, Decomposition of polycyclic aromatic hydrocarbons in atmospheric aqueous droplets through sulfate anion radicals: an experimental and theoretical study, *Science of the Total Environment* 393 (2008) 64–71.
- [23] A. Mills, M. Valenzuela, The photo-oxidation of water by sodium persulfate, and other electron acceptors, sensitized by  $\text{TiO}_2$ , *Journal of Photochemistry and Photobiology A: Chemistry* 165 (2004) 25–34.
- [24] C.A. Martínez-Huitle, E. Brillas, Decontamination of wastewater containing synthetic organic dyes by electrochemical methods: a general review, *Applied Catalysis B: Environmental* 87 (2009) 105–145.
- [25] P. Neta, R.E. Huie, A.B. Ross, Rate constants for reactions of organic radicals in aqueous solution, *Journal of Physical and Chemical Reference Data* 17 (1998) 1027–1284.
- [26] G. Anipsitakis, D. Dionysiou, M. Gonzalez, Cobalt-mediated activation of peroxymonosulfate and sulfate radical attack on phenolic compounds. Implication of chloride ions, *Journal of Physical and Chemical Reference Data* 40 (2006) 1000–1007.
- [27] G. Anipsitakis, D. Dionysiou, Degradation of organic contaminants in water with sulfate radicals generated by the conjunction of peroxymonosulfate with cobalt, *Environmental Science & Technology* 37 (2003) 4790–4797.
- [28] M. Antoniou, A. de la Cruz, D. Dionysiou, Degradation of microcystin-LR using sulfate radicals generated through photolysis, thermolysis and  $e^-$  transfer mechanisms, *Applied Catalysis B: Environmental* 96 (2010) 290–298.
- [29] S. Yang, P. Wang, X. Yang, G. Wei, W. Zhang, L. Shan, A novel advanced oxidation process to degrade organic pollutants in wastewater: microwave-activated persulfate oxidation, *Journal of Environmental Sciences* 21 (2009) 1175–1180.
- [30] J. Zhao, Y. Zhang, X. Quan, S. Chen, Enhanced oxidation of 4-chlorophenol using sulfate radicals generated from zero-valent iron and peroxodisulfate at ambient temperature, *Separation and Purification Technology* 71 (2010) 302–307.
- [31] X.-R. Xu, X.-Z. Li, Degradation of azo dye Orange G in aqueous solutions by persulfate with ferrous ion, *Separation and Purification Technology* 72 (2010) 105–111.
- [32] C. Galindo, P. Jacques, A. Kalt, Photodegradation of the aminoazobenzene acid orange 52 by three advanced oxidation processes: UV/ $\text{H}_2\text{O}_2$ , UV/ $\text{TiO}_2$  and VIS/ $\text{TiO}_2$ : comparative mechanistic and kinetic investigations, *Journal of Photochemistry and Photobiology A: Chemistry* 130 (2000) 35–47.
- [33] V. Kavitha, K. Palanivelu, Degradation of 2-chlorophenol by Fenton and photo-Fenton processes – a comparative study, *Hazardous Substances & Environmental Engineering* 38 (2003) 1215–1231.
- [34] M. Karmaz, E. Puzenat, C. Guillard, J.M. Herrmann, Photocatalytic degradation of the alimentary azo dye amaranth mineralization of the azo group to nitrogen, *Applied Catalysis B: Environmental* 51 (2004) 183–194.
- [35] T.H. Bui, M. Karmaz, E. Puzenat, C. Guillard, J.M. Herrmann, Solar purification and potabilization of water containing dyes, *Research on Chemical Intermediates* 33 (2007) 421–431.
- [36] R. Matta, K. Hanna, S. Chiron, Oxidation of phenol by green rust and hydrogen peroxide at neutral pH, *Separation and Purification Technology* 61 (2008) 442–446.
- [37] A. Kumar, P. Kumar, S. Chand, Catalytic wet peroxide oxidation of azo dye (Congo Red) using modified Zeolite as catalyst, *Journal of Hazardous Materials* 166 (2009) 342–347.
- [38] M. Cheng, W. Song, W. Ma, Ch. Chen, J. Zhao, J. Lin, H. Zhu, Catalytic activity of iron species in layered clays photodegradation of organic dyes under visible irradiation, *Applied Catalysis B-Environmental* 77 (2008) 355–363.
- [39] B. Ahmed, H. Mohamed, E. Limem, B. Nasr, Degradation and mineralization of organic pollutants contained in actual pulp and paper mill wastewater by a UV/ $\text{H}_2\text{O}_2$  process, *Industrial & Engineering Chemistry Research* 48 (2009) 3370–3379.
- [40] S. Su, S.X. Lu, W.G. Xu, Photocatalytic degradation of reactive brilliant blue X-BR in aqueous solutions using quantum-sized ZnO, *Materials Research Bulletin* 43 (2008) 2172–2178.
- [41] I. Bouzaida, C. Ferronato, J.M. Chovelon, M.E. Rammah, J.M. Herrmann, Heterogeneous photocatalytic degradation of the anthraquinonic dye, Acid Blue 25 (AB25): a kinetic approach, *Journal of Photochemistry and Photobiology A: Chemistry* 168 (2004) 23–30.
- [42] N. Stock, J. Peller, K. Vinodgopal, P. Kamat, Combinative sonolysis and photocatalysis for textile dye degradation, *Environmental Science & Technology* 34 (2000) 1747–1750.
- [43] N. Mahmoodi, M. Arami, N. Limaee, N. Tabrizi, Decolorization and aromatic ring degradation kinetics of Direct Red 80 by UV oxidation in the presence of hydrogen peroxide utilizing  $\text{TiO}_2$  as a photocatalyst, *Chemical Engineering Journal* 112 (2005) 191–196.
- [44] J. Fu, Y. Zhao, Q. Wu, Optimizing photoelectrocatalytic oxidation of fulvic acid using response surface methodology, *Journal of Hazardous Materials* 144 (2007) 499–505.
- [45] M.D. Sleiman, D. Vildozo, C. Ferronato, J.M. Chovelon, Photocatalytic degradation of azo dye Metanil Yellow: optimization and kinetic modelling using a chemometric approach, *Applied Catalysis B: Environmental* 77 (1) (2007) 1–11.